


Arsenic Directs Stem Cell Fate by Imparting Notch Signaling Into the Extracellular Matrix Niche

Teresa Anguiano,^{*} Amrita Sahu,[†] Baoli Qian,^{*} Wan-Yee Tang,^{*} Fabrisia Ambrosio,^{*,†,‡,§} and Aaron Barchowsky ^{*,¶,1}

^{*}Department of Environmental and Occupational Health, [†]Department of Physical Medicine and Rehabilitation, [‡]McGowan Institute for Regenerative Medicine, [§]Department of Bioengineering, and [¶]Department of Pharmacology and Chemical Biology, University of Pittsburgh, Pittsburgh, Pennsylvania 15261

¹To whom correspondence should be addressed at Department of Environmental and Occupational Health, University of Pittsburgh, Public Health Room 4133, 130 De Soto Street, Pittsburgh, PA 15261. E-mail: aab20@pitt.edu.

ABSTRACT

Compromise of skeletal muscle metabolism and composition may underlie the etiology of cardiovascular and metabolic disease risk from environmental arsenic exposures. We reported that arsenic impairs muscle maintenance and regeneration by inducing maladaptive mitochondrial phenotypes in muscle stem cells (MuSC), connective tissue fibroblasts (CTF), and myofibers. We also found that arsenic imparts a dysfunctional memory in the extracellular matrix (ECM) that disrupts the MuSC niche and is sufficient to favor the expansion and differentiation of fibrogenic MuSC subpopulations. To investigate the signaling mechanisms involved in imparting a dysfunctional ECM, we isolated skeletal muscle tissue and CTF from mice exposed to 0 or 100 µg/l arsenic in their drinking water for 5 weeks. ECM elaborated by arsenic-exposed CTF decreased myogenesis and increased fibrogenic/adipogenic MuSC subpopulations and differentiation. However, treating arsenic-exposed mice with SS-31, a mitochondrially targeted peptide that repairs the respiratory chain, reversed the arsenic-promoted CTF phenotype to one that elaborated an ECM supporting normal myogenic differentiation. SS-31 treatment also reversed arsenic-induced Notch1 expression, resulting in an improved muscle regeneration after injury. We found that persistent arsenic-induced CTF Notch1 expression caused the elaboration of dysfunctional ECM with increased expression of the Notch ligand DLL4. This DLL4 in the ECM was responsible for misdirecting MuSC myogenic differentiation. These data indicate that arsenic impairs muscle maintenance and regenerative capacity by targeting CTF mitochondria and mitochondrially directed expression of dysfunctional regulators in the stem cell niche. Therapies that restore muscle cell mitochondria may effectively treat arsenic-induced skeletal muscle dysfunction and compositional decline.

Key words: arsenic; Notch; mitochondria; signal transduction; SS-31; extracellular matrix myogenesis; fibrogenesis; adipogenesis; environmental toxicology.

The World Health Organization estimates that disease burden is increased in more than 200 million people worldwide who are exposed to arsenic concentrations in drinking water exceeding the threshold of 10 µg/l (Bailey *et al.*, 2016). Chronic arsenic exposure increases the risk of developing a number of cancers and noncancer diseases that include cardiovascular and metabolic diseases (Kuo *et al.*, 2017; Moon *et al.*, 2017). In addition, arsenic exposures contribute to adverse health outcomes that include skeletal muscle weakness, mobility dysfunction, and impaired

muscle metabolism (Mazumder and Dasgupta, 2011; Parvez *et al.*, 2011).

Skeletal muscle tissue accounts for 40%–50% of body weight in lean individuals and approximately 50% of metabolism. Loss of lean body mass and muscle quality are increasingly recognized as significant risks, if not etiological factors for cardiovascular, lung, and metabolic disease (Correa-de-Araujo *et al.*, 2017; Prado *et al.*, 2018). Muscle quality is critically important to overall well-being, as increased fibrosis and adiposity

(fibro-adipogenesis, myosteatorsis) are associated with an elevated risk of all-cause and cardiovascular disease mortality (Miljkovic-Gacic et al., 2005; Miljkovic and Zmuda, 2010; Santanasto et al., 2017). Increased inter- and intramyocellular fat is an early sign of insulin resistance and impaired metabolism (Goodpaster et al., 2000; Sell et al., 2006; Vigouroux et al., 2011). As awareness of the importance of muscle quality decline and myosteatorsis in the etiology and promotion of disease has only recently increased (Aleixo et al., 2020; Nachit and Leclercq, 2019; Prado et al., 2018), few studies have investigated environmental influences on muscle decline and myosteatorsis. Nonetheless, a limited number of epidemiological (Parvez et al., 2011) and animal studies (Ambrosio et al., 2014; Garciafigueroa et al., 2013; Yen et al., 2010; Zhang et al., 2016) found that environmental arsenic exposure impairs skeletal muscle function and promotes ectopic fat deposition, dysfunctional metabolism, dysfunctional myogenesis, and aberrant progenitor cell differentiation.

Skeletal muscle is composed of highly metabolic, insulin sensitive fibers, as well as neural and vascular structures, elaborate networks of connective tissue and extracellular matrix (ECM), and multiple stem/progenitor cell populations (Moyle et al., 2019; Tedesco et al., 2010, 2017). Although the primary role of the ECM is to provide structural support required for motor function, it is also an essential repository for cellular communications and helps to regulate metabolic functions (Hays et al., 2008; Zhang et al., 2016). The ECM is predominantly generated by connective tissue fibroblasts (CTF) and vascular-associated cells, and it provides the regulatory niche for resident stem cells (Gillies and Lieber, 2011). Disrupting the interactions within these resident cell populations and modifying their molecular contributions to the ECM microenvironment compromises the balance within the skeletal muscle niche, including its overall structure and metabolism (Engler et al., 2006; Smith et al., 2017; Stearns-Reider et al., 2017; Williams et al., 2015; Zhang et al., 2016).

We have previously shown that human muscle stem cells (hMuSC) cultured on decellularized ECM constructs derived from arsenic-exposed skeletal muscle, undergo a fibrogenic conversion unlike hMuSC cultured on control ECM constructs (Zhang et al., 2016). These data confirm that hMuSC are receptive to signaling from the skeletal muscle ECM and suggest that arsenic exposure imparts changes within the ECM that misdirect hMuSC differentiation. Furthermore, CTF isolated from arsenic-exposed mice (CTF^{ars}) retain elevated NF- κ B-driven ECM gene transcript levels, relative to CTF isolated from control mice (CTF^{ctr}) (Zhang et al., 2016), and these levels may promote ECM remodeling and dysfunctional ECM to cell communications. We also found that arsenic targets mitochondrial morphology and dynamics to disrupt muscle metabolism, mitochondrial oxidant generation, and epigenetic memory in muscle progenitor cells (Ambrosio et al., 2014; Cheikhi et al., 2019, 2020). Thus, in this study, we investigated whether arsenic effects on CTF mitochondria underlie dysfunctional elaboration of a stress memory into the ECM. Given that signaling from this memory may also direct muscle stem cells (MuSC) fate and impair muscle maintenance and regenerative capacity, we also investigated the signaling mechanisms involved in imparting the CTF^{ars} ECM memory that reduces myogenesis and drives fibro-adipogenic differentiation of hMuSC.

MATERIALS AND METHODS

Animal exposures. Six-week-old male C57Bl/6J mice (Jackson Laboratory) were exposed to 0 or 100 sodium meta-arsenite

(NaAsO₂; Fisher Scientific) in their drinking water for 5 weeks, at which time the mice were euthanized and hind limb muscles collected. Arsenite was used as it is the most environmentally relevant toxic form of inorganic arsenic in drinking water. We found that this exposure causes pathological tissue and ECM remodeling in multiple organs of the mouse without causing any signs of overt lethality or changes in weight gain (Ambrosio et al., 2014; Garciafigueroa et al., 2013; Soucy et al., 2005; Straub et al., 2008; Zhang et al., 2016). Fresh arsenite-containing water was provided every 2 and 3 days to ensure that there is little arsenite oxidation to pentavalent arsenate. All studies were approved by the Institutional Animal Care and Use Committee of the University of Pittsburgh. As shown in the scheme in Figure 3A, in experiments evaluating SS-31 for reversing arsenic effects, arsenic exposure was stopped after 5 weeks, and the mice received daily ip injections of SS-31 (1 mg/kg in saline) or saline for 1 week. Bilateral tibialis anterior (TA) muscles were then injured with 20 μ l of 1.2% (w/v) barium chloride (BaCl₂). The mice were allowed to recover for 2 weeks, and after euthanizing, TA muscles were evaluated for tissue regeneration, gastrocnemius muscles were collected for gene transcript and ChIP analysis, and CTF were isolated from the remaining hind limb muscles.

CTF isolation. For each isolation, CTF were isolated from hind limb muscles of 2 mice, essentially as described (Goetsch et al., 2015). After euthanizing the mice, hind limb muscles were removed and finely minced in Hank's balanced salt solution (HBSS). The minced pieces were collected by centrifugation at 900 \times g for 5 min, resuspended in Collagenase XI (2 mg/ml in HBSS C7657 Sigma Aldrich), and digested for 60 min at 37°C with shaking every 10 min. The suspension was centrifuged for 5 min at 900 \times g and the supernatant was discarded. The pellet was resuspended in dispase II (2.4 U/ml in HBSS, ThermoFisher 17105041) and digested for 45 min at 37°C with shaking every 10 min. The suspension was again centrifuged for 5 min at 900 \times g, the supernatant was discarded, and the pellet was resuspended in 0.1% Trypsin. After a 30-min incubation followed by centrifugation, the resulting cell pellet was resuspended in growth medium (DMEM [4.5 g glucose/ml] supplemented with 10% fetal bovine serum [Hyclone], 10% horse serum [Hyclone], 1% penicillin-streptomycin antibiotics and 0.5% chicken essential extract). The suspension was filtered through a 70 micron strainer and the cells in the filtrate were seeded in collagen-coated 6-well plates. Nonadherent cells were removed after 3 h and the adherent CTFs were cultured in fresh growth medium. Greater than 95% of the adhered CTF^{ctr} and CTF^{ars} stained positive for the fibroblast marker, α -smooth muscle actin (α SMA).

CTF ECM elaboration, decellularization, and myoblast differentiation. Primary CTF were seeded onto collagen-coated 8-well glass chamber slides (10 000 cells/well) and allowed to elaborate an ECM for 2 and 3 days. The ECM was decellularized by incubating the wells with HBSS at room temperature for 10 min and then in distilled water for 1 h. The slides were then rinsed 3 times with HBSS until all the cells and cell ghosts were removed. hMuSC (ScienCell No. 3510) were seeded onto the decellularized ECM construct at 10 000 cells/well and differentiated for 2 days by culturing in differentiation medium (DMEM [4.5 g/l glucose] supplemented with 2% Horse Serum [Hyclone] and 1% penicillin-streptomycin). At the end of the differentiation period, the cultures were fixed and prepared for immunofluorescent imaging.

To examine the effect of inhibiting CTF^{ctr} and CTF^{ars} Notch on hMuSC differentiation on the elaborated ECM, DAPT (1 μ M) was added to CTF 1 day after seeding and for an additional 2 days of ECM elaboration. DAPT was removed by decellularizing and rinsing the ECM prior to seeding hMuSC. To demonstrate the role of ECM DLL4, the elaborated ECM was coated with antibody (1 μ g/ml) for 3 h at 37°C. The antibody solution was rinsed away prior to seeding hMuSC for differentiation.

Quantitative immunofluorescence imaging. CTF^{ctr} and CTF^{ars} were seeded on coated 8-well chamber glass slides and cultured until near confluence. hMuSC were seeded on ECM elaborated onto the glass slides and cultured in differentiation medium for 2 days. At the end of the experimental period for both cell types, the cells were then fixed with 2% paraformaldehyde for 15 min at room temperature, washed 3 times with PBS, and permeabilized with 0.1% Triton X-100 in PBS for 15 min at room temperature. Slides were then washed 3 times with PBS and 5 times with PBS + 0.5% BSA (PBB). Slides were subsequently blocked with 5% natural donkey serum (Millipore S30-100KC) diluted in PBB for 60 min, washed 5 times with PBB, and then incubated with primary antibodies (Supplementary Table 1: list of antibodies and dilutions) for 60 min at room temperature. After 5 washes with PBB, the slides were incubated with fluorophore-conjugated secondary antibodies (Supplementary Table 1) for 60 min, washed 5 times with PBB, 3 times with PBS, and stained with 4',6-diamidino-2-phenylindole (BioLegend 422801) for 1 min. After mounting coverslips with Fluoromount-G (eBiosciences 004958-02), the slides were imaged using a Nikon A1 confocal microscope (University of Pittsburgh Center for Biologic Imaging). At least 3 microscopic fields were imaged per culture. The mean fluorescent intensity of each protein (desmin, NICD, PDGFR α , and CD34) was quantified using Nikon Elements AR software (Nikon). Intensity of MyoD with in cell nuclei was calculated and averaged per field of view.

Transmission electron microscopy. CTF grown in coated 12-well plastic plates were fixed in 2.5% glutaraldehyde in 100 mM PBS (8 gm/l NaCl, 0.2 gm/l KCl, 1.15 gm/l Na₂HPO₄·7H₂O, 0.2 gm/l KH₂PO₄, pH 7.4) overnight at 4°C. Monolayers were washed 3 times with PBS and then postfixed in aqueous 1% osmium tetroxide, 1% Fe₆CN₃ for 1 h. After 3 washes with PBS, the cells were dehydrated through a 30%–100% ethanol series and then several changes of Polybed 812 embedding resin (Polysciences, Warrington, Pennsylvania). Cultures were embedded in by inverting Polybed 812-filled BEEM capsules on top of the cells. Blocks were cured overnight at 37°C, and then cured for 2 days at 65°C. Monolayers were pulled off the coverslips and re-embedded for cross section. Ultrathin cross sections (60 nm) of the cells were obtained on a Reichert Ultracut E microtome, poststained in 4% uranyl acetate for 10 min and in 1% lead citrate for 7 min. Sections were imaged using a JEM 1011 TEM (JEOL, Peabody, Massachusetts) at 80 kV. Images were taken using a side-mount AMT 2k digital camera (Advanced Microscopy Techniques, Danvers, Massachusetts).

Second harmonics generation imaging of whole mount muscles. Second harmonics generation (SHG) imaging of intact TA muscles was performed as we previously described. Briefly, after 2 weeks of recovery from BaCl₂ injury, TAs were excised, placed in 2% paraformaldehyde for 2 h, and then in Scaleview solution (Olympus) for at least 1 week. Scaleview solution was replenished every 3 days. The samples were rinsed and stored in PBS at 4°C until imaged. All imaging was performed with an

Olympus multiphoton microscope (Model FV1000, ASW software, Tokyo, Japan). Prior to imaging, samples were placed in hanging drop slides in PBS and a cover slip was placed over the well and in contact with the muscle. The muscle was oriented with the superior border aligned parallel to the superior edge of the slide and the dorsal surface of the muscle against the cover slip. Images were taken of the medial and lateral muscle bellies at the site of injury to a depth of 100 μ m, with a step thickness of 2 μ m and a scan pixel count of 1024 \times 1024.

Western analysis. Western analyses for changes in OXPHOS complex protein abundance were performed, as previously described (Barchowsky et al., 1999; Klei et al., 2013). Briefly, CTF cultures were lysed in RIPA buffer containing protease, kinase, and phosphates inhibitors, and homogenized by sonication. After centrifugation at 10 000 \times g for 5 min at 4°C, protein content of the supernatant was determined by BCA assay (ThermoFisher) and the remainder of the supernatant was mixed with 6X Laemmli sample loading buffer. Equal amounts of protein were separated by PAGE and transferred to PDVF membranes (Immobilon-IF, EMD Millipore Corporation, Billerica, Massachusetts). After blocking, the membranes were incubated with Total OXPHOS Rodent WB Antibody Cocktail (Abcam No. ab110413) and antibody to voltage-dependent anion channel (VDAC) (Abcam No. ab15895), rinsed, and then incubated with IRDye 800CW Donkey anti-Mouse IgG or IRDye 680LT Donkey anti-Rabbit IgG (Li-COR Biosciences), respectively. Digital infrared imaging and quantification of the protein bands was performed using a LI-COR Odyssey Clx imager and Image Studio v5.2 software.

Gene transcript and ChIP analysis. Gastrocnemius muscles were snap frozen in liquid nitrogen and RNA was isolated from pulverized tissue powder using the AllPrep DNA/RNA/miRNA Universal Kit (Qiagen, Germantown, Maryland). Isolated RNA was reverse transcribed using iScript gDNA Clear cDNA Synthesis Kit (BIO-RAD, Hercules, California). Notch1 mRNA levels were quantified by SYBR Green-based real-time PCR (qPCR) using SsoAdvanced Universal SYBR Green Supermix (BIO-RAD). Transcript levels were normalized to the expression level of Rpl44, and the fold changes of Notch1 relative to universal mouse reference RNA (Qiagen) were calculated using 2- $\Delta\Delta$ Ct method. Each sample was measured in duplicate. Primers sequence: Rpl44 (Forward: 5'-AGATGAGGCAGAGGTCCAA-3', Reverse: 5'-GTTGTAAAGAAAGGCGGTCA-3') and Notch1 (Forward: 5'-ACAGTGCAACCCCTGTATG-3', Reverse: 5'-TCTAGGCCATCCCCTCACA-3'). For ChIP analysis, pulverized tissue powder was fixed with 1% formaldehyde for 15 min followed by quenching with 125-mM glycine solution. Cross-linked proteins were pelleted and washed with PBS containing protease inhibitor cocktail. Chromatin isolation and immunoprecipitation was performed using ChIP-IT kit (Active Motif, Carlsbad, California), following the manufacturer's instructions. One to 2 micrograms of ChIP-validated antibodies against RNA Polymerase II (A2032, Epigentek, Farmingdale, New York), or H2A.Zac (ab18262, Abcam, Cambridge, Massachusetts) were used for immunoprecipitation of each sample. One percent of nonimmunoprecipitated chromatin was used as input. Following reverse crosslinking and elution of chromatin, DNA from each sample was purified with QIAquick PCR purification kit (Qiagen). Ten nanograms of purified DNA was used for PCR of the 5' promoter region of Notch1 (-107 to +90 nt) using the primers: forward: 5'-CACAAGGGGTAAGGGTTC-3' and Reverse:

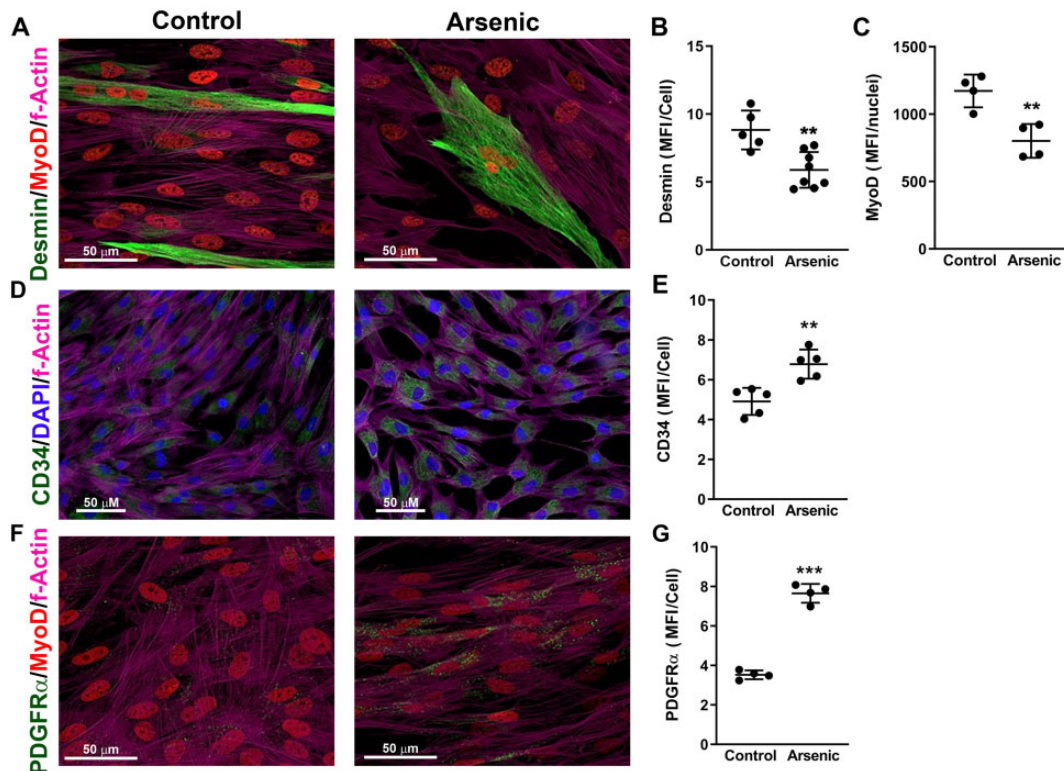


Figure 1. Extracellular matrix (ECM) from connective tissue fibroblasts (CTF) isolated from arsenic-exposed mice (CTF^{ars}) inhibits myogenesis and promotes fibro-adipogenic differentiation. Hind limb muscle CTF were isolated from control mice (CTF^{ctr}) and mice exposed for 5 weeks to 100 μ g/l arsenic in drinking water (CTF^{ars}). The CTF were seeded in the absence of arsenic and allowed to elaborate matrix for 3 days. The cells were removed, and unexposed human muscle stem cells were cultured on the elaborated ECM in differentiation medium for 2 days. Cells were fixed and immunostained for the indicated proteins, as well as stained for nuclei (4',6-diamidino-2-phenylindole, DAPI) and actin filaments (phalloidin). Immunofluorescence in $\times 40$ or $\times 60$ magnification confocal images was quantified and the data are presented as mean and SEM of the mean fluorescence intensity (MFI) per cell or nuclei captured in individual microscopic fields (images from 3 replicate cultures representative of cultures isolated from at least 4 mice per treatment). Statistical differences were determined by unpaired t tests (** $p < .01$, *** $p < .001$).

5'-GGCTCGTTCCTTCACTGC-3'. The percent of immunoprecipitated DNA relative to the input was calculated.

Statistical analysis. Data in graphs are expressed as mean \pm SEM. Significance between groups was determined by Student's t tests or 1-way ANOVA followed by either Dunnett's or Tukey's test for multiple comparisons. *A priori*, differences were considered to be significantly different at $p < .05$. Statistical analysis and graphing were performed using GraphPad Prism v8.3.1 software.

RESULTS

ECM Elaborated From Arsenic-exposed CTF Impairs Myogenic Differentiation

We previously found that environmentally relevant exposure to arsenic (100 μ g/l: 2–5 weeks) in drinking water impairs skeletal muscle maintenance and injury repair (Ambrosio et al., 2014; Zhang et al., 2016). A 100 μ g/l in drinking water is not an uncommon human exposure and is approximately the EC90 we found for arsenic promoted remodeling of mouse liver vasculature in this mouse model (Ambrosio et al., 2014; Garciafigueroa et al., 2013; Soucy et al., 2005; Straub et al., 2007, 2008; Zhang et al., 2016). Although exact translation of this exposure to the human equivalent is difficult, allometric scaling (FDA, 2005) would estimate this to be a human exposure of approximately 20 μ g/l or twice the WHO/EPA safe drinking water level. CTF^{ars} retained aberrant expression of ECM proteins when cultured in the

absence of arsenic, and arsenic exposure caused decellularized ECM scaffolds to direct naïve heterogenic hMuSC populations toward fibrogenic instead of myogenic differentiation (Zhang et al., 2016). To test the functional consequence of the aberrant ECM elaborated by the CTF^{ars}, we seeded CTF isolated from the hind limb muscles of control or arsenic-exposed (100 μ g/l: 5 weeks) mice and allowed them to elaborate matrix for 2 and 3 days. The cells were then removed, and hMuSC, not exposed to arsenic, were cultured in myogenic differentiation medium on the elaborated matrix for 2 days. As seen in Figures 1A–C, myogenic differentiation, as determined by MyoD and desmin expression, was reduced in hMuSC seeded on ECM elaborated by CTF^{ars} when compared with hMuSC seeded onto ECM from CTF^{ctr}. In contrast, the hMuSC seeded on the CTF^{ars} ECM had increased expression of both the proliferation marker CD34 (Figs. 1D and 1E) and fibro-adipogenic marker PDGFR α (Figs. 1F and 1G).

Arsenic Targets CTF Mitochondria to Impair Myogenesis and Muscle Regeneration

The fact that the CTF^{ars} elaborated a pathogenic ECM even when cultured in the absence of arsenic suggests that the cells retained an epigenetic-driven memory of the arsenic stress, as we found in MuSC isolated from arsenic-exposed mice and in myogenic cell lines exposed to arsenic in culture (Ambrosio et al., 2014; Cheikhi et al., 2019). Specifically, we showed that the regulation of this memory was directed by dysfunctional mitochondria (Cheikhi et al., 2019). The CTF^{ars} possessed the same

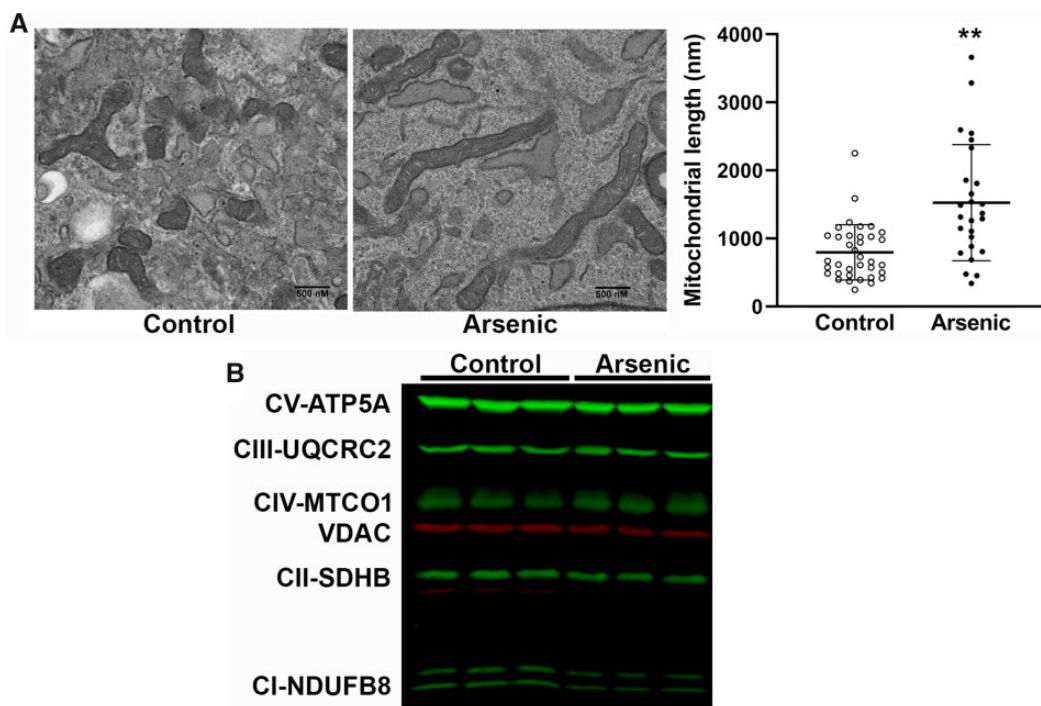


Figure 2. Arsenic effects on connective tissue fibroblasts (CTF) mitochondrial morphology and respiratory complexes. **A**, CTF^{ctr} and CTF^{ars} isolated from 2 mice per treatment were cultured in the absence of arsenic for 3 days and then fixed and processed for imaging at $\times 25\,000$ magnification by transmission electron microscopy. The length of mitochondria in 3–4 separate images was measured using Image J software (dots are individual mitochondria). Statistical significance between groups was determined by unpaired t test (** $p < .01$). **B**, CTF^{ctr} and CTF^{ars} from 2 mice per treatment were amplified in culture and total protein was probed for expression of mitochondrial respiratory complexes by immunoblotting (second blot presented in [Supplementary Figure 2](#)). The abundance of respiratory complex proteins (green) and VDAC (red) are given in [Table 1](#). Abbreviation: VDAC, voltage-dependent anion channel.

Table 1. Abundance of CTF Mitochondrial Channel and Respiratory Proteins

Protein	Control	Arsenic	Arsenic/Control
Complex V (ATP5A)	4320 \pm 480.6	3477 \pm 430.3	0.80 \pm 0.08
Complex IV (MTCO1)	1385 \pm 74.0	1285 \pm 51.8	0.89 \pm 0.06
Complex III (UQCRC2)	1144 \pm 64.7	983.0 \pm 66.8	0.86 \pm 0.04
Complex II (SDHB)	1044 \pm 25.0	789.0 \pm 36.2 ^a	0.75 \pm 0.03 ^b
Complex I (NDUFB8)	374.2 \pm 16.7	271.7 \pm 4.8 ^a	0.73 \pm 0.03 ^b
VDAC	41 717 \pm 1831	31 567 \pm 725.1 ^a	0.75 \pm 0.02 ^b

Data are mean \pm SEM of relative Infrared band intensity or fold intensity relative to control.

^aDesignates significant difference ($p < .001$) between cells from control and arsenic mice ($n = 6$) as determined by an unpaired t test.

^bDesignates significant difference ($p < .05$) from the fold control abundance of Complex IV ($n = 6$) as determined by an unpaired t test.

Abbreviations: CTF, connective tissue fibroblasts; VDAC, voltage-dependent anion channel.

elongated mitochondrial networks with disrupted cristae ([Figure 2A](#)) that we found in arsenic-exposed muscle tissue, MuSC, and myocytes ([Ambrosio et al., 2014](#); [Cheikhi et al., 2019](#)). Despite the apparent increase in large fused mitochondria, there was an approximately 25% loss of respiratory Complex I and Complex II proteins, as well as the (VDAC) protein in CTF^{ars} relative to other respiratory complex proteins and relative to levels in control CTF ([Figure 2B](#) and [Table 1](#)).

SS-31 is a mitochondrially targeted peptide that binds cardiolipin and cardiolipin-associated proteins to preserve or restore respiratory chain function ([Campbell et al., 2019](#); [Szeto and Liu, 2018](#)). We have demonstrated that SS-31, and other

mitochondrial protectant compounds, reverse arsenic effects on myocyte mitochondrial function and epigenetic regulation ([Cheikhi et al., 2019, 2020](#)). To test whether repairing the respiratory chain could revert the CTF^{ars} phenotype *in vivo*, mice were treated with SS-31 for 1 week after stopping arsenic exposure. The mice then received bilateral injections of BaCl₂ in their TA muscles to produce a defined myofiber injury and were allowed to recover for 2 weeks ([Figure 3A](#): experimental paradigm). As seen in [Figures 3B–D](#), SS-31 treatments reversed the effects of the arsenic exposure as CTF^{ars} isolated from SS-31-treated mice (CTF^{ars/SS-31}) elaborated a matrix with the same myogenic instruction as that elaborated by CTF^{ctr}. It should be noted that ECM from CTF^{ctr/SS-31} had a negative effect that was equivalent to ECM from CTF^{ars}. Regardless, the SS-31 treatment only slightly impaired *in vivo* regeneration of injured TA myofibers (number of centrally nucleated regenerating fibers and myotube fusion index), but completely reversed arsenic-inhibited repair ([Figs. 3E–G](#)).

Arsenic-stimulated Notch Signaling Mediates Dysfunctional Repair and ECM Elaboration

Notch proteins are master regulators of cell fate. Continuous Notch signaling in muscle inhibits myogenesis, but promotes fibro-adipogenic differentiation of muscle progenitors cells ([Brack et al., 2008](#); [Buas and Kadesch, 2010](#); [Kitzmann et al., 2006](#); [Marinkovic et al., 2019](#); [Pasut et al., 2016](#); [Verma et al., 2018](#)). In screening for regulatory gene changes in the uninjured gastrocnemius muscles of the groups of mice shown in [Figure 4](#), we found that arsenic induced a sustained increase in Notch1 expression, and that SS-31 treatment returned Notch1 mRNA to control expression levels ([Figure 4A](#)). Notch1 expression

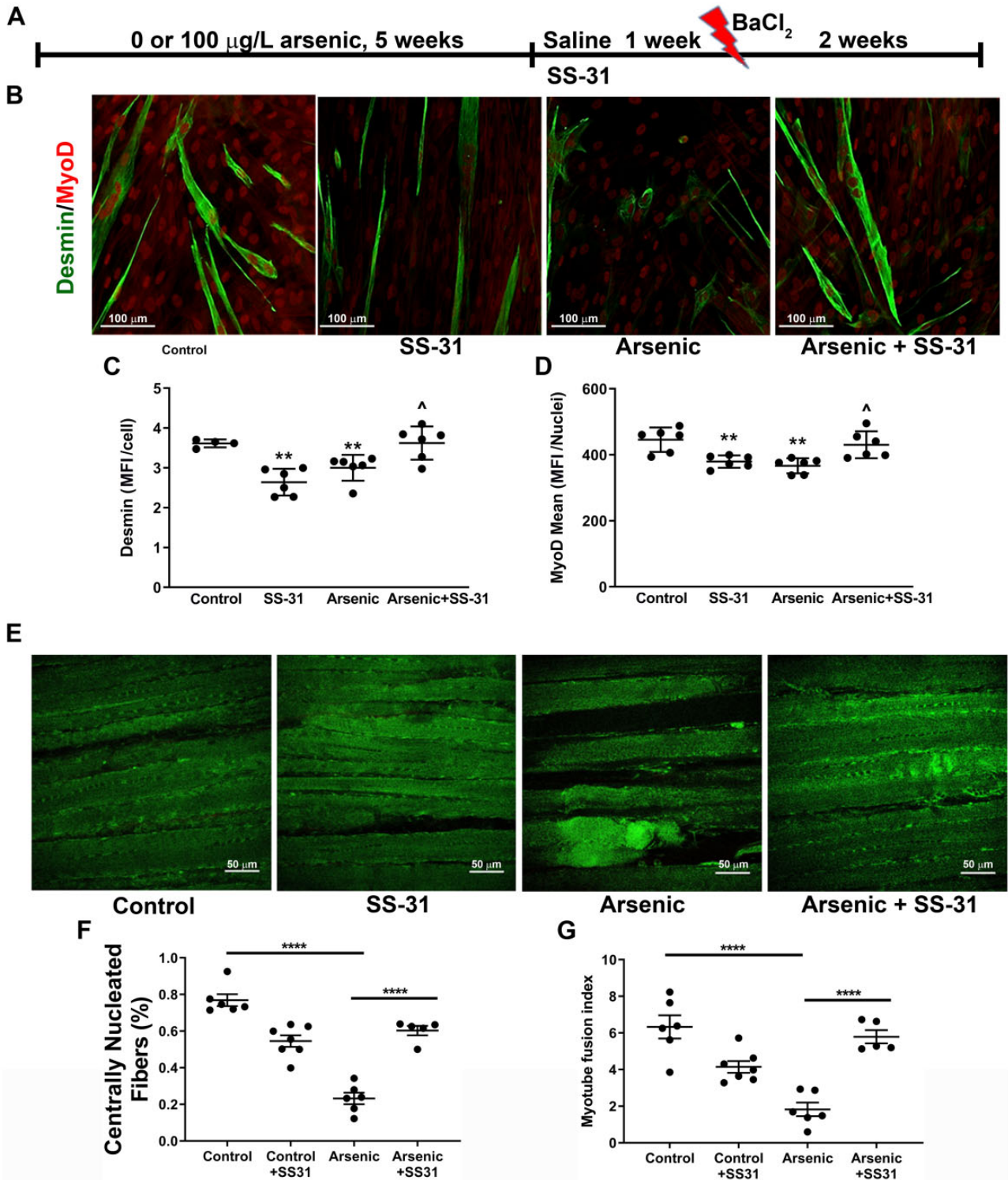


Figure 3. Mitochondrial SS-31 treatment reverses arsenic effects on extracellular matrix (ECM) and regeneration. **A**, Experimental scheme and timeline for mouse exposure, SS-31 intervention and tibialis anterior (TA) injury. **B**, Myofiber differentiation (**C** desmin-positive structures and **D** nuclear MyoD expression) of unexposed human muscle stem cells (hMuSC) seeded on ECM elaborated from connective tissue fibroblasts (CTF) isolated from control, arsenic, and SS-31 (CTF^{SS-31}, CTF^{ars/SS-31}) mice (6 replicate cultures from 4 mice in each treatment). **E**, Whole TAs were isolated and cleared for second harmonics generation imaging of intact muscle. **F** and **G**, Regenerating centrally nucleated fibers and muscle fiber fusion index were quantified and compared for statistical differences. Mean ± SEM values from 6 mice in each treatment group were compared by 1-way ANOVA followed by Tukey's ad hoc multiple comparison. In **C** and **D** ** designates statistical significance from hMuSC seeded on CTF^{ctr} ECM ($p < .01$) and ^ designates difference from cells seeded on CTF^{ars} ECM ($p < .05$). In **F** and **G**, **** designates difference from control or arsenic ($p < .0001$). Abbreviation: MFI, mean fluorescence intensity.

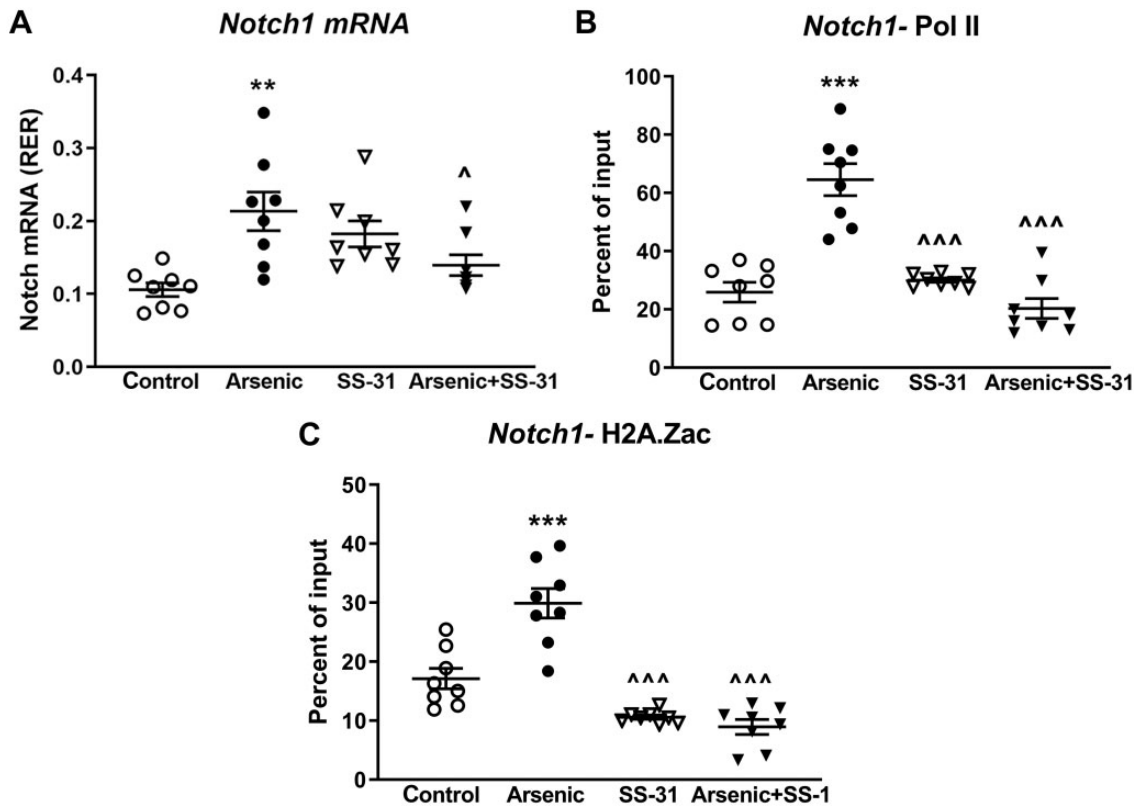


Figure 4. SS-31 reversal of arsenic-induced *Notch1* expression *in vivo*. **A**, Quantitative PCR measure of *Notch1* mRNA levels in uninjured gastrocnemius muscle from the mice in [Figure 3. B and C](#), ChIP analysis of Pol II or H2A.Zac binding at the *Notch1* promoter. Means \pm SD of the treatment groups were compared with 1-way ANOVA followed by Tukey's ad hoc multiple comparison. Significant differences from control are indicated by ** $p < .01$ or *** $p < .001$, and from arsenic by ^ $p < .05$ or ^^ $p < .001$; $n = 8$ mice in each treatment group.

remained elevated 3 weeks after arsenic was removed from the drinking water, suggesting prolonged epigenetic regulatory change. Indeed, ChIP analysis of the *Notch1* promoter revealed that the transcriptional start site was held in an open, RNA polymerase Pol II-bound conformation ([Figure 4B](#)), perhaps driven by the increased binding of the active epigenetic mark, acetylated H2A.Z ([Figure 4C](#)), in muscles from the arsenic-exposed mice. As we previously reported ([Cheikhi et al., 2019](#)), this epigenetic memory was driven by arsenic-promoted mitochondrial dysfunction, because SS-31 treatment reversed arsenic-induced *Notch1* mRNA expression and the binding of active epigenetic marks on the *Notch1* promoter.

To demonstrate that arsenic-induced CTF *Notch1* expression and functionally increased *Notch1* signaling, CTF^{ctrl} and CTF^{ars} were seeded in arsenic-free culture and compared for activated *Notch1* (NICD) protein expression and expression of the NICD-driven *Notch* ligand, DLL4. Quantitative immunofluorescence analysis demonstrated that CTF^{ars} retained elevated NICD levels *ex vivo*, relative to control CTF ([Figs. 5A and 5B](#)). The CTF^{ars} also retained increased expression of DLL4 ([Figs. 5A and 5C](#)). In contrast, CTF^{ars} isolated from mice that received 1 week of SS-31 treatment had NICD and DLL4 levels that were essentially equal to CTF^{ctrl} ([Figs. 5A–C](#)). In addition, treating CTF^{ars} with the γ -secretase inhibitor, DAPT, *ex vivo* reduced both NICD and DLL4 expression. These data suggest arsenic exposure creates an epigenetic memory for enhanced *Notch* signaling in CTFs and that DLL4 expression was downstream of NICD transactivation.

To investigate the functional importance of *Notch1* and NICD-induced DLL4 in arsenic-inhibited myogenesis, CTF^{ctrl} and CTF^{ars} were again seeded to elaborate a matrix. After 1 day,

DAPT was added to groups of the CTF^{ctrl} and CTF^{ars} cultures, and decellularized ECM was prepared on culture day 3. hMuSC were then seeded on the ECM for 2 days in differentiation media. ECM elaborated by CTF^{ars} cultures inhibited generation of desmin-positive fibers myofibers and decreased hMuSC nuclear MyoD levels ([Figs. 6A–C](#)). However, treating the CTF^{ars} with DAPT attenuated the effect of the CTF^{ars} elaborated on hMuSC differentiation. To demonstrate that the effect of DAPT resulted from decreased DLL4 elaboration into the ECM, decellularized ECM from CTF^{ctrl} or CTF^{ars} was incubated with an antibody that blocks DLL4 binding to *Notch*. Unbound antibody was rinsed from the ECM and hMuSC were seeded in differentiation medium. Blocking ECM DLL4 increased hMuSC myogenic differentiation to levels greater than control and more than reversed the effect of the CTF^{ars} phenotype ([Figs. 6D and 6E](#) and [Supplementary Figure 3](#)).

Antibody blocking of DLL4 may have been more effective than DAPT, because the antibody would block both basally expressed and NICD-induced DLL4.

DISCUSSION

Collectively, the data indicate that low-to-moderate arsenic exposure induces functional ECM-associated changes in the MuSC niche, findings that may help explain muscle weakness and metabolic dysfunction experienced by individuals in arsenic-endemic areas. Furthermore, the data implicate arsenic effects on mitochondria in creating prolonged epigenetic signaling for dysfunctional ECM and dysregulated MuSC fate. The study demonstrates that muscle tissue and CTF isolated from mice weeks

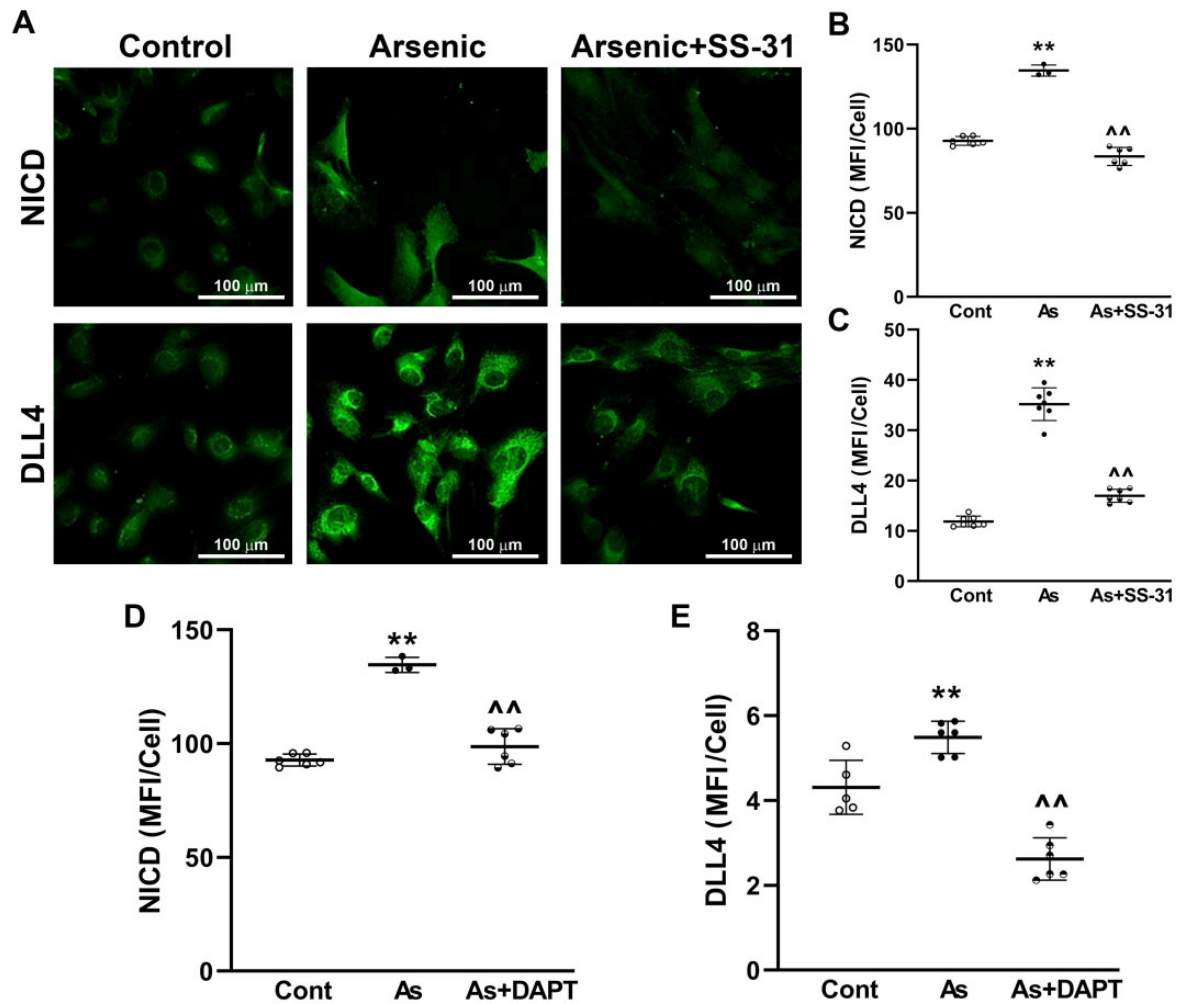


Figure 5. SS-31 reversal of arsenic-induced connective tissue fibroblasts (CTF) Notch1 activity. A–C, CTF were isolated from hind limb muscles (excluding tibialis anterior and gastrocnemius) from the mice in Figure 3 and cultured for 24 h before fixing and quantitative immunofluorescence analysis of activated Notch (NICD) and DLL4 protein expression. D and E, Groups of CTF^{ars} were cultured *ex vivo* with 1 μM DAPT and abundance of NICD and DLL4 was compared with CTF^{ctrl} and CTF^{ars} (note that values for CTF^{ctrl} and CTF^{ars} NICD in B and D are from the same cultures, whereas data in C and E are from separate cultures). Mean ± SEM of the MFI/cell from the groups (cont, control; As, arsenic) were compared using 1-way ANOVA and Tukey’s ad hoc multiple comparison. Significant differences from control are indicated by ***p* < .01 or and from arsenic by ^^*p* < .01.

(1.5–2 human year equivalents) after arsenic exposure was terminated retained elevated Notch1 expression and signaling that misdirected populations of MuSC away from myogenesis and toward fibro-adipogenesis. The CTF^{ars} phenotype was also accompanied by atypical mitochondrial morphology. Intervention with SS-31 reversed arsenic-inhibited tissue regeneration, epigenetic induction of Notch1, and functional impairment from the ECM elaborated by CTF^{ars}. Together, these data implicate aberrant Notch1 signaling as the mechanism for the arsenic-promoted myomatrix remodeling that impairs muscle metabolism, maintenance, and regeneration.

Notch signaling is a key regulator of MuSC quiescence, self-renewal activity, and stem cell fate determinations that promote muscle pathologies (Bjornson et al., 2012; Gerli et al., 2019; Kitzmann et al., 2006). Notch activity represses skeletal muscle myogenesis by preserving MuSC in a proliferative stem cell-like state (eg, increased CD34 expression, Figure 1) while concomitantly reducing the number of CD34-positive reserve cells that fuse to make myotubes (Cappellari et al., 2013; Gerli et al., 2019; Kitzmann et al., 2006). Notch promotes asymmetric MuSC division and divergent fates of daughter cells (Conboy

and Rando, 2002). Over-activation of Notch signaling in skeletal muscle impaired stem cell support of muscle regeneration (Brack et al., 2008) and/or promoted differentiation of subpopulations of MuSC into brown adipocytes (Pasut et al., 2016) or pericytes (Cappellari et al., 2013). While increased DLL4 signaling is sufficient for directing MuSC subpopulations toward pericyte differentiation, maximal transdifferentiation occurs with costimulation by PDGF-BB, a platelet-derived growth factor that activates PDGFRα (Cappellari et al., 2013). Pericytes can be derived from multiple lineages and, as a result, express heterogeneous phenotypes even within the same tissues (Dias Moura Prazeres et al., 2017). The data in Figure 1 suggest that as CTF^{ars}-elaborated ECM reduces hMuSC myogenic differentiation, it enhances a population of cells expressing PDGFRα and αSMA, which are indicative of type 1 pericytes (Birbrair et al., 2013). This is significant because type 1 pericytes are more prone to adipogenic differentiation relative to their myogenic type 2 counterparts (Birbrair et al., 2013) and may underlie the increase in perivascular ectopic adipose tissue that we reported in skeletal muscle of arsenic-exposed mice (Garciafigueroa et al., 2013).

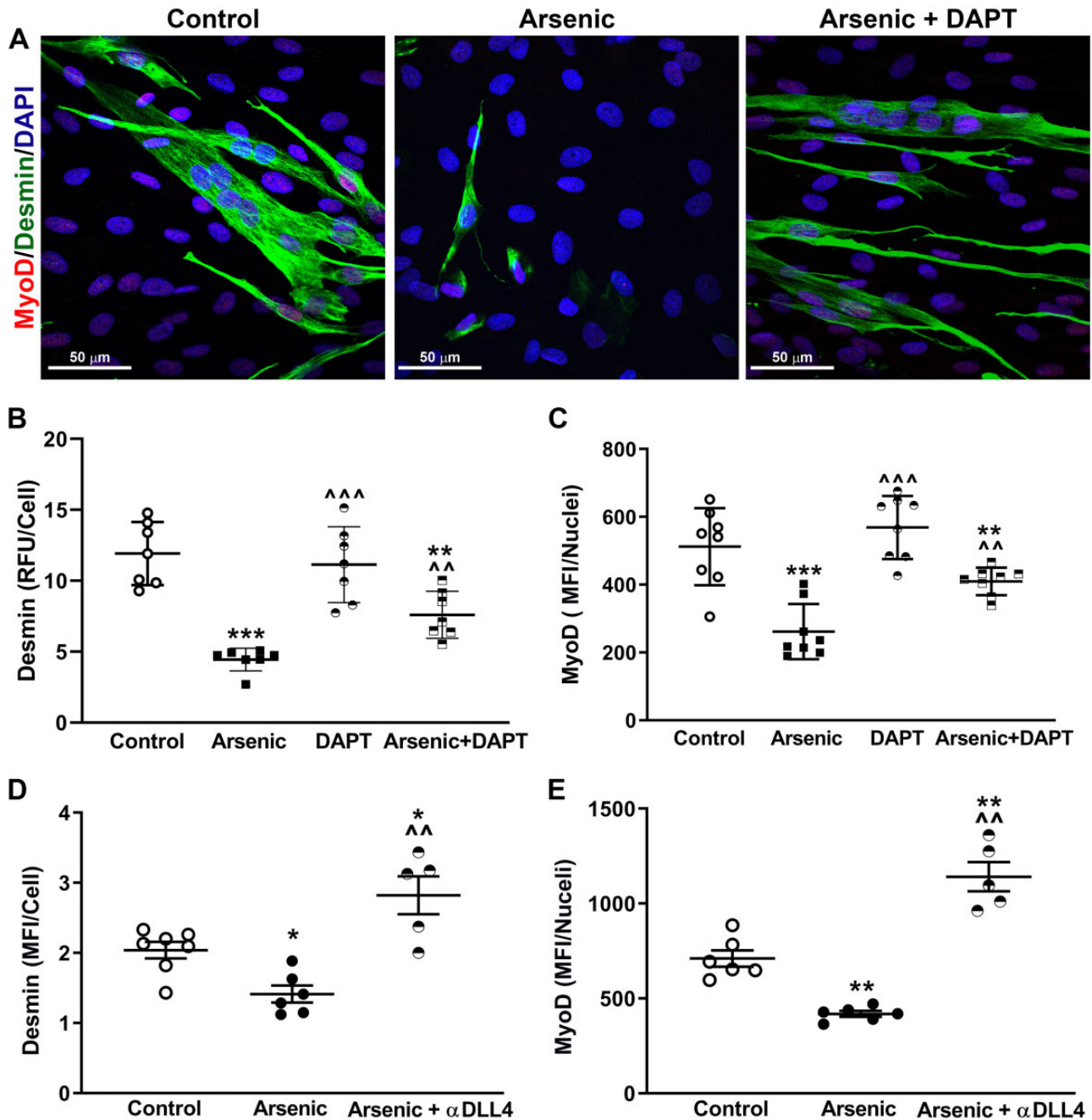


Figure 6. Notch-induced extracellular matrix (ECM) DLL4 impairs hMPC myogenic differentiation. A–C, CTF^{CTT} and CTF^{ARS} were seeded and cultured for 1 day before adding 1 μ M DAPT to the designated groups. On culture day 3, cells were removed and human muscle stem cells (hMuSC) were seeded on elaborated ECM and cultured in differentiation medium for 2 days before fixing and quantifying desmin and nuclear MyoD expression. D and E, CTF^{CTT} and CTF^{ARS} were cultured for 3 days to elaborate ECM. The cells were removed and the ECM was incubated with an antibody that blocks DLL4/Notch binding. After rinsing to remove unbound antibody, hMuSC were seeded and cultured in differentiation medium for 2 days before fixing and quantifying desmin and nuclear MyoD expression. Mean \pm SEM expression from the groups were compared using 1-way ANOVA and Tukey's ad hoc multiple comparison. Significant differences from CTF^{CTT} ECM are indicated by * $p < .05$, ** $p < .01$, or *** $p < .001$ and from CTF^{ARS} ECM by $\sim p < .01$ or $\sim\sim p < .001$.

Notch signaling is initiated when the membrane-bound ligands of the Delta-like (DLL1, DLL3, DLL4) and the Jagged (JAG1 and JAG2) families engage and transactivate Notch receptors on neighboring cells (Buas and Kadesch, 2010; Wakabayashi et al., 2015). Notch signaling is essential for MuSC quiescence, health, and expansion of myogenic progenitors in postnatal myogenesis and regeneration (Bjornson et al., 2012; Brack et al., 2008; Conboy et al., 2003). However, myogenic differentiation requires

a temporal switch from Notch signaling to cell-cell transactivation of Wnt/ β -catenin signaling. Sustained NICD or DLL4 signaling, such as observed from the CTF^{ARS}-elaborated ECM, prevents this transition and directs the fibro-adipogenic and pericytes differentiation of MuSC populations (Cappellari et al., 2013; Moyle et al., 2019; Pasut et al., 2016). The novel observation that CTF^{ARS}-elaborated DLL4 is essentially a memory of arsenic-promoted stress imparted into the ECM and that it continues to

direct pathogenic tissue remodeling, even after arsenic has been removed, is significant. It has important implications for the impacts of chronic arsenic exposures on muscle maintenance and regenerative capacity. It is also consistent with our previous demonstration that decellularized muscle ECM scaffolds isolated from arsenic-exposed mice caused hMuSC to be redirected to a fibrogenic determination rather than their normal myogenic fate (Zhang et al., 2016). It appears that, without intervention such as SS-31 administration, the pathogenic ECM, and epigenetic memory of arsenic exposures persists. However, it remains unclear whether or when these memories may ultimately be spontaneously erased. The data in Figures 3 and 4 suggest that this reversal could occur years after human arsenic exposure is terminated.

The successful *in vivo* reversal of arsenic-inhibited tissue regeneration and Notch signaling resulting from SS-31 treatment confirms our previous findings that arsenic targets mitochondria to impart the persistent epigenetic memory of stress (Ambrosio et al., 2014; Cheikhi et al., 2019). Arsenic-promoted mitochondrial respiratory chain dysfunction and possibly mitochondrial oxidants appear to be upstream of epigenetic control of genes regulating DNA and chromatin methylation and acetylation (Cheikhi et al., 2019; Cronican et al., 2013) and Notch1/DLL4 signaling in skeletal muscle (Figure 4). Mitochondrial dynamics and ROS generation have been placed upstream of Notch expression and signaling in a range of stem cells with implications on their homeostasis and fate (Paul et al., 2014; Wakabayashi et al., 2015). However, Notch signaling has also been shown to affect mitochondrial function, as it inhibits mitochondrial complex 1 by repressing expression of multiple *Nduf* subunit transcripts (Lee and Long, 2018). The arsenic-promoted decrease in mitochondrial complexes 1 and 2 (Figure 2B and Table 1) would be consistent with a reciprocal feed-forward dysregulation of mitochondrial signaling and Notch activation. The memory of this dysregulation may be manifest in the enhanced binding of epigenetic marks in the *Notch1* promoter, such as the increased acetylation and DNA binding of H2A.Zac that may be promoted by decreased deacetylase substrate NAD⁺ (decreased complex 1) or increased acetylase substrate acetylCoA (dysfunctional complex 2) (Shaughnessy et al., 2014; Wallace and Fan, 2010; Weinhouse, 2017).

The axis of oxidative stress leading to Notch expression is strongly linked through activation of the Nrf2 (nuclear factor, erythroid factor 2, type 2) transcription factor, as the *Notch1* promoter contains Nrf2 responsive ARE cis-elements (Wakabayashi et al., 2015). However, this is not a linear relationship as the NICD affects Nrf2 expression and both transcription factors can elicit feedback mechanisms on the respective signaling pathways (Wakabayashi et al., 2015). It is important to note that Nrf2 appears to be essential for the regenerative response of muscle, as well as lung tissue, and that induction of Notch may be a portion of this essentiality (Paul et al., 2014; Shelar et al., 2016; Wakabayashi et al., 2015). However, Nrf2 is also important for limiting the increased flux of ROS that is critical for initiating Notch signaling, stem cell self-renewal and tissue regeneration, as excessive ROS impairs these temporal transitions (Paul et al., 2014; Shelar et al., 2016). Arsenical effects on mitochondria are very effective in activating myocyte antioxidant responses (Cheikhi et al., 2019) and the data in Figures 5 and 6 suggest that chronic activation may be linked to loss of temporal *Notch1* regulation both through cell-autonomous and ECM signaling. However, the data in Figure 4 also suggest that mitochondrial-driven epigenetic regulation may contribute to or bypass the Nrf2 axis of *Notch1* regulation.

In summary, this study demonstrated that arsenic exposure impairs muscle regeneration by eliciting chronic mitochondrial-driven activation of Notch signaling at the level of fibroblast elaboration of ECM-bound NICD-induced DLL4. This DLL4 is a memory of arsenic-promoted stress imparted into the ECM that pathogenically misdirects the fate of the heterogeneous MuSC populations. Remarkably, the memory of arsenic exposure is held both in mitochondrial-driven epigenetic regulation and cell elaborated transactivating ligands. As Notch signaling is activated in resident MuSC populations of the skeletal muscle niche, subpopulations are disproportionately activated to proliferate and overwhelmingly advance nonmyogenic/adipogenic cells that decrease regenerative integrity and contribute to decline of muscle metabolism and tissue integrity.

SUPPLEMENTARY DATA

Supplementary data are available at *Toxicological Sciences* online.

FUNDING

National Institute of Environmental Health Sciences (R01ES023696, R01ES025529 to F.A. and A.B.); National Institute on Aging (R01AG061005 to F.A.). We acknowledge the National Institutes of Health-supported microscopy resources in the Center for Biologic Imaging (1S10OD019973-01).

DECLARATION OF CONFLICTING INTERESTS

The authors declared no potential conflicts of interest with respect to the research, authorship, and/or publication of this article.

REFERENCES

- Aleixo, G. F. P., Shachar, S. S., Nyrop, K. A., Muss, H. B., Malpica, L., and Williams, G. R. (2020). Myosteatosis and prognosis in cancer: Systematic review and meta-analysis. *Crit. Rev. Oncol. Hematol.* **145**, 102839.
- Ambrosio, F., Brown, E., Stolz, D., Ferrari, R., Goodpaster, B., Deasy, B., Distefano, G., Roperti, A., Cheikhi, A., Garciafigueroa, Y., et al. (2014). Arsenic induces sustained impairment of skeletal muscle and muscle progenitor cell ultrastructure and bioenergetics. *Free Radic. Biol. Med.* **74**, 64–73.
- Bailey, K. A., Smith, A. H., Tokar, E. J., Graziano, J. H., Kim, K. W., Navasumrit, P., Ruchirawat, M., Thiantanawat, A., Suk, W. A., and Fry, R. C. (2016). Mechanisms underlying latent disease risk associated with early-life arsenic exposure: Current research trends and scientific gaps. *Environ. Health Perspect.* **124**, 170–175.
- Barchowsky, A., Roussel, R. R., Klei, L. R., James, P. E., Ganju, N., Smith, K. R., and Dudek, E. J. (1999). Low levels of arsenic trioxide stimulate proliferative signals in primary vascular cells without activating stress effector pathways. *Toxicol. Appl. Pharmacol.* **159**, 65–75.
- Birbrair, A., Zhang, T., Wang, Z. M., Messi, M. L., Enikolopov, G. N., Mintz, A., and Delbono, O. (2013). Role of pericytes in skeletal muscle regeneration and fat accumulation. *Stem Cells Dev.* **22**, 2298–2314.
- Bjornson, C. R., Cheung, T. H., Liu, L., Tripathi, P. V., Steeper, K. M., and Rando, T. A. (2012). Notch signaling is necessary to

- maintain quiescence in adult muscle stem cells. *Stem Cells* **30**, 232–242.
- Brack, A. S., Conboy, I. M., Conboy, M. J., Shen, J., and Rando, T. A. (2008). A temporal switch from notch to Wnt signaling in muscle stem cells is necessary for normal adult myogenesis. *Cell Stem Cell* **2**, 50–59.
- Buas, M. F., and Kadesch, T. (2010). Regulation of skeletal myogenesis by Notch. *Exp. Cell Res.* **316**, 3028–3033.
- Campbell, M. D., Duan, J., Samuelson, A. T., Gaffrey, M. J., Merrihew, G. E., Egertson, J. D., Wang, L., Bammler, T. K., Moore, R. J., White, C. C., et al. (2019). Improving mitochondrial function with SS-31 reverses age-related redox stress and improves exercise tolerance in aged mice. *Free Radic. Biol. Med.* **134**, 268–281.
- Cappellari, O., Benedetti, S., Innocenzi, A., Tedesco, F. S., Moreno-Fortuny, A., Ugarte, G., Lampugnani, M. G., Messina, G., and Cossu, G. (2013). Dll4 and PDGF-BB convert committed skeletal myoblasts to pericytes without erasing their myogenic memory. *Dev. Cell* **24**, 586–599.
- Cheikhi, A., Anguiano, T., Lasak, J., Qian, B., Sahu, A., Mimiya, H., Cohen, C. C., Wipf, P., Ambrosio, F., and Barchowsky, A. (2020). Arsenic stimulates myoblast mitochondrial EGFR to impair myogenesis. *Toxicol. Sci.* kfaa031. doi: 10.1093/toxsci/kfaa031
- Cheikhi, A., Wallace, C., St Croix, C., Cohen, C., Tang, W. Y., Wipf, P., Benos, P. V., Ambrosio, F., and Barchowsky, A. (2019). Mitochondria are a substrate of cellular memory. *Free Radic. Biol. Med.* **130**, 528–541.
- Conboy, I. M., Conboy, M. J., Smythe, G. M., and Rando, T. A. (2003). Notch-mediated restoration of regenerative potential to aged muscle. *Science* **302**, 1575–1577.
- Conboy, I. M., and Rando, T. A. (2002). The regulation of Notch signaling controls satellite cell activation and cell fate determination in postnatal myogenesis. *Dev. Cell* **3**, 397–409.
- Correa-de-Araujo, R., Harris-Love, M. O., Miljkovic, I., Fragala, M. S., Anthony, B. W., and Manini, T. M. (2017). The need for standardized assessment of muscle quality in skeletal muscle function deficit and other aging-related muscle dysfunctions: A symposium report. *Front. Physiol.* **8**, 87.
- Cronican, A. A., Fitz, N. F., Carter, A., Saleem, M., Shiva, S., Barchowsky, A., Koldamova, R., Schug, J., and Lefterov, I. (2013). Genome-wide alteration of histone H3K9 acetylation pattern in mouse offspring prenatally exposed to arsenic. *PLoS One* **8**, e53478.
- Dias Moura Prazeres, P. H., Sena, I. F. G., Borges, I. D. T., de Azevedo, P. O., Andreotti, J. P., de Paiva, A. E., de Almeida, V. M., de Paula Guerra, D. A., Pinheiro Dos Santos, G. S., Mintz, A., et al. (2017). Pericytes are heterogeneous in their origin within the same tissue. *Dev. Biol.* **427**, 6–11.
- Engler, A. J., Sen, S., Sweeney, H. L., and Discher, D. E. (2006). Matrix elasticity directs stem cell lineage specification. *Cell* **126**, 677–689.
- FDA. (2005). *Estimating the Maximum Safe Starting Dose in Initial Clinical Trials for Therapeutics in Adult Healthy Volunteers* (C. f. D. E. Research, Ed.), pp. 1–27. Washington, DC.
- Garciafigueroa, D. Y., Klei, L. R., Ambrosio, F., and Barchowsky, A. (2013). Arsenic-stimulated lipolysis and adipose remodeling is mediated by G-protein-coupled receptors. *Toxicol. Sci.* **134**, 335–344.
- Gerli, M. F. M., Moyle, L. A., Benedetti, S., Ferrari, G., Ucuncu, E., Ragazzi, M., Constantinou, C., Louca, I., Sakai, H., Ala, P., et al. (2019). Combined Notch and PDGF Signaling enhances migration and expression of stem cell markers while inducing perivascular cell features in muscle satellite cells. *Stem Cell Rep.* **12**, 461–473.
- Gillies, A. R., and Lieber, R. L. (2011). Structure and function of the skeletal muscle extracellular matrix. *Muscle Nerve* **44**, 318–331.
- Goetsch, K. P., Snyman, C., Myburgh, K. H., and Niesler, C. U. (2015). Simultaneous isolation of enriched myoblasts and fibroblasts for migration analysis within a novel co-culture assay. *Biotechniques* **58**, 25–32.
- Goodpaster, B. H., Thaete, F. L., and Kelley, D. E. (2000). Thigh adipose tissue distribution is associated with insulin resistance in obesity and in type 2 diabetes mellitus. *Am. J. Clin. Nutr.* **71**, 885–892.
- Hays, A. M., Lantz, R. C., Rodgers, L. S., Sollome, J. J., Vaillancourt, R. R., Andrew, A. S., Hamilton, J. W., and Camenisch, T. D. (2008). Arsenic-induced decreases in the vascular matrix. *Toxicol. Pathol.* **36**, 805–817.
- Kitzmann, M., Bonnien, A., Duret, C., Vernus, B., Barro, M., Laoudj-Chenivresse, D., Verdi, J. M., and Carnac, G. (2006). Inhibition of Notch signaling induces myotube hypertrophy by recruiting a subpopulation of reserve cells. *J. Cell. Physiol.* **208**, 538–548.
- Klei, L. R., Garciafigueroa, D. Y., and Barchowsky, A. (2013). Arsenic activates endothelin-1 Gi protein-coupled receptor signaling to inhibit stem cell differentiation in adipogenesis. *Toxicol. Sci.* **131**, 512–520.
- Kuo, C. C., Moon, K. A., Wang, S. L., Silbergeld, E., and Navas-Acien, A. (2017). The association of arsenic metabolism with cancer, cardiovascular disease, and diabetes: A systematic review of the epidemiological evidence. *Environ. Health Perspect.* **125**, 087001.
- Lee, S. Y., and Long, F. (2018). Notch signaling suppresses glucose metabolism in mesenchymal progenitors to restrict osteoblast differentiation. *J. Clin. Invest.* **128**, 5573–5586.
- Marinkovic, M., Fuoco, C., Sacco, F., Cerquone Perpetuini, A., Giuliani, G., Micarelli, E., Pavlidou, T., Petrilli, L. L., Reggio, A., Riccio, F., et al. (2019). Fibro-adipogenic progenitors of dystrophic mice are insensitive to NOTCH regulation of adipogenesis. *Life Sci. Alliance* **2**, e201900437.
- Mazumder, D. G., and Dasgupta, U. B. (2011). Chronic arsenic toxicity: Studies in West Bengal, India. *Kaohsiung J. Med. Sci.* **27**, 360–370.
- Miljkovic-Gacic, I., Ferrell, R. E., Patrick, A. L., Kammerer, C. M., and Bunker, C. H. (2005). Estimates of African, European and Native American ancestry in Afro-Caribbean men on the island of Tobago. *Hum. Hered.* **60**, 129–133.
- Miljkovic, I., and Zmuda, J. M. (2010). Epidemiology of myosteato-sis. *Curr. Opin. Clin. Nutr. Metab. Care* **13**, 260–264.
- Moon, K. A., Oberoi, S., Barchowsky, A., Chen, Y., Guallar, E., Nachman, K. E., Rahman, M., Sohel, N., D'Ippoliti, D., Wade, T. J., et al. (2017). A dose-response meta-analysis of chronic arsenic exposure and incident cardiovascular disease. *Int. J. Epidemiol.* **46**, 1924–1939.
- Moyle, L. A., Tedesco, F. S., and Benedetti, S. (2019). Pericytes in muscular dystrophies. *Adv. Exp. Med. Biol.* **1147**, 319–344.
- Nachit, M., and Leclercq, I. A. (2019). Emerging awareness on the importance of skeletal muscle in liver diseases: Time to dig deeper into mechanisms! *Clin. Sci.* **133**, 465–481.
- Parvez, F., Wasserman, G. A., Factor-Litvak, P., Liu, X., Slavkovich, V., Siddique, A. B., Sultana, R., Sultana, R., Islam, T., Levy, D., et al. (2011). Arsenic exposure and motor function among children in Bangladesh. *Environ. Health Perspect.* **119**, 1665–1670.

- Pasut, A., Chang, N. C., Rodriguez, U. G., Faulkes, S., Yin, H., Lacaria, M., Ming, H., and Rudnicki, M. A. (2016). Notch signaling rescues loss of satellite cells lacking Pax7 and promotes brown adipogenic differentiation. *Cell Rep.* **16**, 333–343.
- Paul, M. K., Bisht, B., Darmawan, D. O., Chiou, R., Ha, V. L., Wallace, W. D., Chon, A. T., Hegab, A. E., Grogan, T., Elashoff, D. A., et al. (2014). Dynamic changes in intracellular ROS levels regulate airway basal stem cell homeostasis through Nrf2-dependent Notch signaling. *Cell Stem Cell* **15**, 199–214.
- Prado, C. M., Purcell, S. A., Alish, C., Pereira, S. L., Deutz, N. E., Heyland, D. K., Goodpaster, B. H., Tappenden, K. A., and Heymsfield, S. B. (2018). Implications of low muscle mass across the continuum of care: A narrative review. *Ann. Med.* **50**, 675–693.
- Santanasto, A. J., Goodpaster, B. H., Kritchevsky, S. B., Miljkovic, I., Satterfield, S., Schwartz, A. V., Cummings, S. R., Boudreau, R. M., Harris, T. B., and Newman, A. B. (2017). Body composition remodeling and mortality: The health aging and body composition study. *J. Gerontol. A Biol. Sci. Med. Sci.* **72**, 513–519.
- Sell, H., Dietze-Schroeder, D., and Eckel, J. (2006). The adipocytomyocyte axis in insulin resistance. *Trends Endocrinol. Metab.* **17**, 416–422.
- Shaughnessy, D. T., McAllister, K., Worth, L., Haugen, A. C., Meyer, J. N., Domann, F. E., Van Houten, B., Mostoslavsky, R., Bultman, S. J., Baccarelli, A. A., et al. (2014). Mitochondria, energetics, epigenetics, and cellular responses to stress. *Environ. Health Perspect.* **122**, 1271–1278.
- Shelar, S. B., Narasimhan, M., Shanmugam, G., Litovsky, S. H., Gounder, S. S., Karan, G., Arulvasu, C., Kensler, T. W., Hoidal, J. R., Darley-Usmar, V. M., et al. (2016). Disruption of nuclear factor (erythroid-derived-2)-like 2 antioxidant signaling: A mechanism for impaired activation of stem cells and delayed regeneration of skeletal muscle. *FASEB J.* **30**, 1865–1879.
- Smith, L., Cho, S., and Discher, D. E. (2017). Mechanosensing of matrix by stem cells: From matrix heterogeneity, contractility, and the nucleus in pore-migration to cardiogenesis and muscle stem cells *in vivo*. *Sem. Cell Dev. Biol.* **71**, 84–98.
- Soucy, N. V., Mayka, D., Klei, L. R., Nemecek, A. A., Bauer, J. A., and Barchowsky, A. (2005). Neovascularization and angiogenic gene expression following chronic arsenic exposure in mice. *Cardiovasc. Toxicol.* **5**, 29–41.
- Stearns-Reider, K. M., D'Amore, A., Beezhold, K., Rothrauff, B., Cavalli, L., Wagner, W. R., Vorp, D. A., Tsamis, A., Shinde, S., Zhang, C., et al. (2017). Aging of the skeletal muscle extracellular matrix drives a stem cell fibrogenic conversion. *Aging Cell* **16**, 518–528.
- Straub, A. C., Clark, K. A., Ross, M. A., Chandra, A. G., Li, S., Gao, X., Pagano, P. J., Stolz, D. B., and Barchowsky, A. (2008). Arsenic-stimulated liver sinusoidal capillarization in mice requires NADPH oxidase-generated superoxide. *J. Clin. Invest.* **118**, 3980–3989.
- Straub, A. C., Stolz, D. B., Vin, H., Ross, M. A., Soucy, N. V., Klei, L. R., and Barchowsky, A. (2007). Low level arsenic promotes progressive inflammatory angiogenesis and liver blood vessel remodeling in mice. *Toxicol. Appl. Pharmacol.* **222**, 327–336.
- Szeto, H. H., and Liu, S. (2018). Cardiolipin-targeted peptides rejuvenate mitochondrial function, remodel mitochondria, and promote tissue regeneration during aging. *Arch. Biochem. Biophys.* **660**, 137–148.
- Tedesco, F. S., Dellavalle, A., Diaz-Manera, J., Messina, G., and Cossu, G. (2010). Repairing skeletal muscle: Regenerative potential of skeletal muscle stem cells. *J. Clin. Invest.* **120**, 11–19.
- Tedesco, F. S., Moyle, L. A., and Perdiguero, E. (2017). Muscle interstitial cells: A brief field guide to non-satellite cell populations in skeletal muscle. *Methods Mol. Biol.* **1556**, 129–147.
- Verma, M., Asakura, Y., Murakonda, B. S. R., Pengo, T., Latroche, C., Chazaud, B., McLoon, L. K., and Asakura, A. (2018). Muscle satellite cell cross-talk with a vascular niche maintains quiescence via VEGF and Notch signaling. *Cell Stem Cell* **23**, 530–543.e9.
- Vigouroux, C., Caron-Debarle, M., Le Dour, C., Magre, J., and Capeau, J. (2011). Molecular mechanisms of human lipodystrophies: From adipocyte lipid droplet to oxidative stress and lipotoxicity. *Int. J. Biochem. Cell Biol.* **43**, 862–876.
- Wakabayashi, N., Chartoumpakis, D. V., and Kensler, T. W. (2015). Crosstalk between Nrf2 and Notch signaling. *Free Radic. Biol. Med.* **88**, 158–167.
- Wallace, D. C., and Fan, W. (2010). Energetics, epigenetics, mitochondrial genetics. *Mitochondrion* **10**, 12–31.
- Weinhouse, C. (2017). Mitochondrial-epigenetic crosstalk in environmental toxicology. *Toxicology* **391**, 5–17.
- Williams, A. S., Kang, L., and Wasserman, D. H. (2015). The extracellular matrix and insulin resistance. *Trends Endocrinol. Metab.* **26**, 357–366.
- Yen, Y. P., Tsai, K. S., Chen, Y. W., Huang, C. F., Yang, R. S., and Liu, S. H. (2010). Arsenic inhibits myogenic differentiation and muscle regeneration. *Environ. Health Perspect.* **118**, 949–956.
- Zhang, C., Ferrari, R., Beezhold, K., Stearns-Reider, K., D'Amore, A., Haschak, M., Stolz, D., Robbins, P. D., Barchowsky, A., and Ambrosio, F. (2016). Arsenic promotes NF- κ B-mediated fibroblast dysfunction and matrix remodeling to impair muscle stem cell function. *Stem Cells* **34**, 732–742.